551. 501. 777
551. 511. 23
551. 513. 11
551. 558. 2

DIVERGENCE, VERTICAL VELOCITY AND CONVERSION BETWEEN POTENTIAL AND KINETIC ENERGY IN AN EXTRATROPICAL DISTURBANCE[1])

by

E. PALMÉN and E. O. HOLOPAINEN[2])

Academy of Finland, Helsinki

Abstract

For a selected synoptic situation characterized by a deepening cyclone over the central parts of the U.S. the field of divergence and the corresponding vertical velocities have been computed by using the continuity equation for standard isobaric surfaces up to 300 mb. In the principal precipitation region of the cyclone the divergence values are also used for an estimate of the amount of precipitation, and it has been shown that there is a satisfactory agreement between the observed and computed amounts of rainfall if sufficiently large regions are considered.

From the field of vertical velocity the rate of conversion between potential and kinetic energy is evaluated. For the same region also the net flux of kinetic energy across the horizontal and vertical boundaries, the work done by the surrounding atmosphere and the dissipation of energy due to friction are estimated and compared with the change of kinetic energy inside the region.

---

[1]) The research has been carried out under a Contract Nonr-1143 (00) between Woods Hole Oceanographic Institution, U.S.A. and the International Meteorological Institute, Stockholm.

[2]) Present affiliation: International Meteorological Institute, Stockholm.

1. Introduction

During recent years several attempts have been made to evaluate the large-scale field of divergence and vertical velocity associated with cyclonic and anticyclonic disturbances by using observed winds [4]. One of the purposes of these attempts has been to find out whether the regular synoptic wind data are sufficiently exact to permit a satisfactory evaluation of divergence and vertical velocity. Since the vertical component of the air movement determines the conversion between potential and kinetic energy in the atmosphere and is essential for most weather

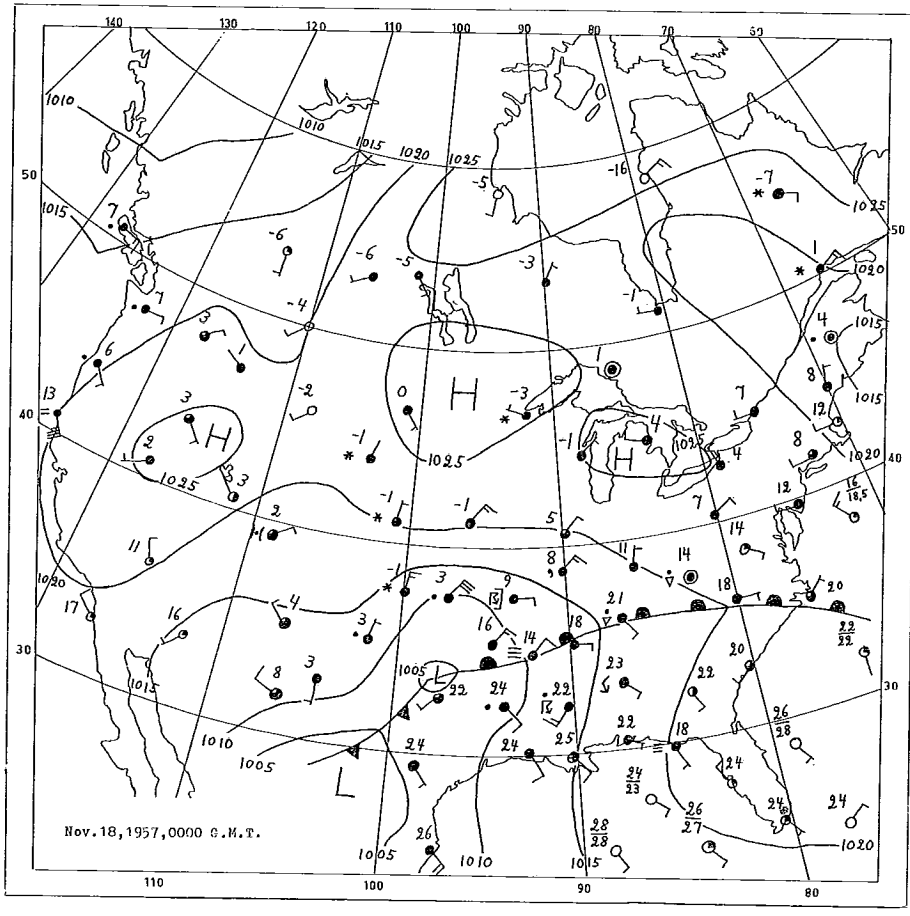

Fig. 1.

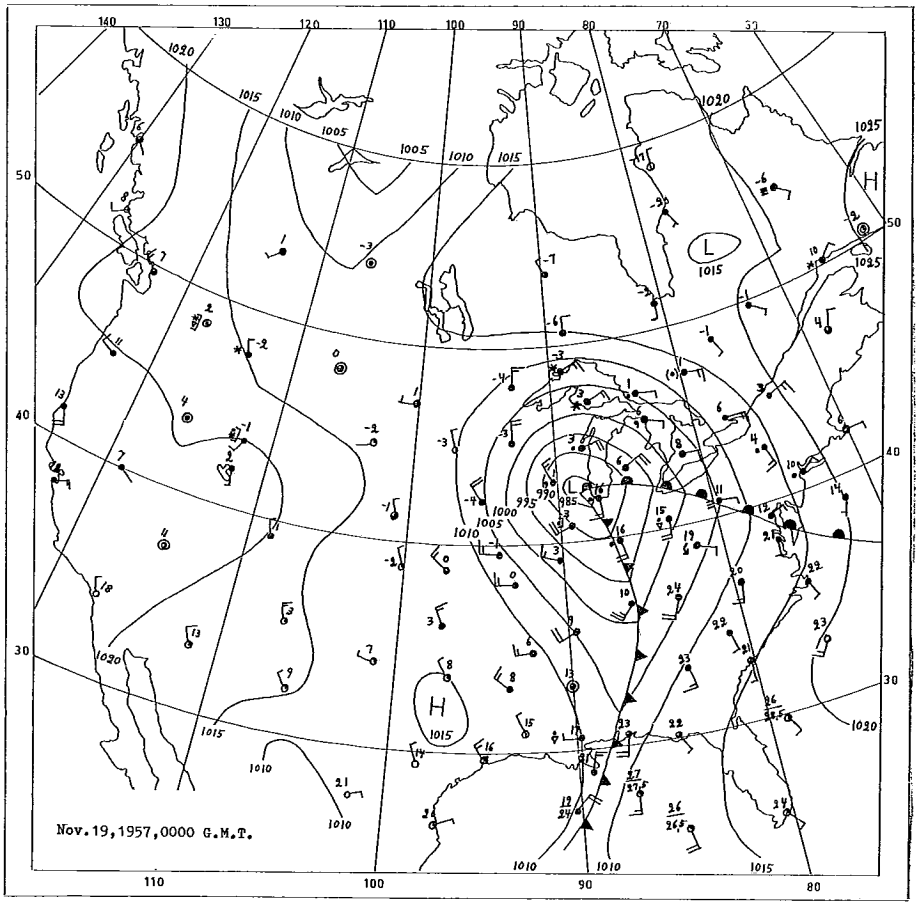

Fig. 2.

phenomena, a correct computation of the field of vertical velocity must be considered extremely important in the dynamic and synoptic meteorology.

Due to the relatively sparse net-work of wind stations over large parts of the earth it may be difficult to extend computations of this type to cover considerable regions of the globe. Also, considering the small magnitude of the vertical wind components in comparison with the total wind velocity, satisfactory results can primarily be expected in regions with the best possible wind observations and in synoptic situations in which relatively strong vertical velocities occur. To this type of syn-

optic situations belong in the first place deepening cyclones accompanied by intense precipitation over sufficiently large areas. Very valuable informations concerning the mechanism of cyclone development and the energy processes involved can be obtained from systematic case studies of this type.

For our case study the deepening cyclone over the central parts of the U.S. on November 18, 1957, 1200 G.M.T. was selected. The center of the surface cyclone over southwestern Missouri had a depth of about 1000 mb and was moving in a northeasterly direction under considerable deepening. The warm and cold fronts of the cyclone were very well

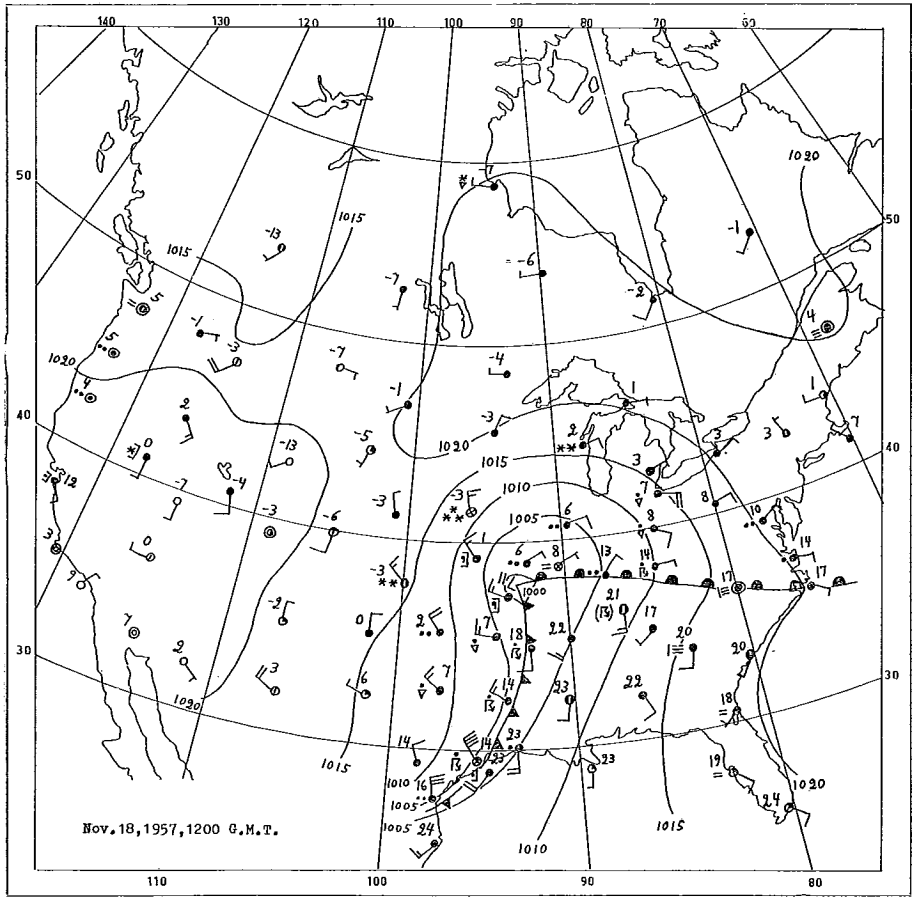

Fig. 3.

marked, and the depression was accompanied by intense rain. The surface development can be seen from the maps for November 18, 0000 and 1200 G.M.T. and November 19, 0000 G.M.T. During this 24 hours period a deepening of about 20 mb occurred. The 500-mb chart in Fig. 4 shows the characteristic features of a developing extratropical disturbance with its cold through surrounded both in the east and west by warmer ridges. The precipitation was not confined only to the frontal zones; also in the central regions of the very distinct warm sector heavy rain of shower type occurred in the unstable tropical air flowing northwards from the Gulf region.

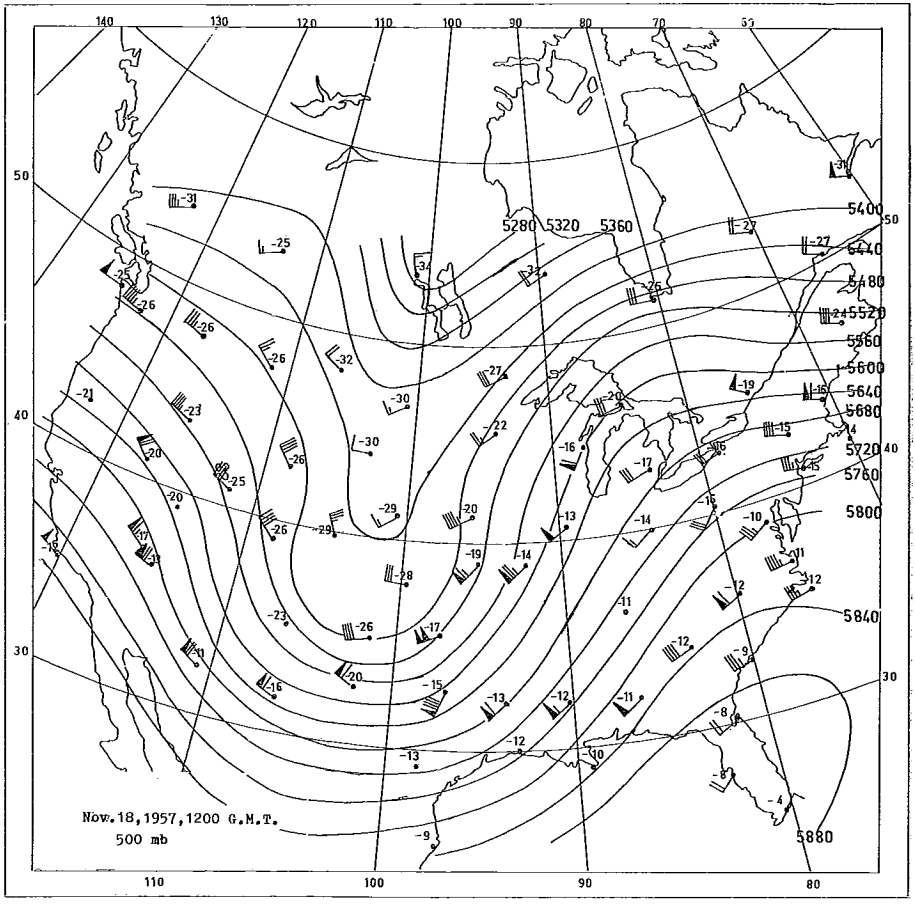

Fig. 4.

2. Method of Computation

For the computation the area limited by the latitudes 33.°75 and 48.°75 N and the longitudes 78.°75 and 118.°75 W was used. In zonal direction the region approximately extended over the whole wave length of the 500-mb disturbance. In meridional direction it would have been better to extend the region somewhat farther south- and northwards, but due to the lack of good upper wind data, especially around latitude 30°N, the meridional width of the area had to be reduced.

The total area, about 5.56×10^{12} m^2 large, was divided into two similar parts by the meridian 98.°75 W, each part being 2.78×10^{12} m^2 in area. The subregions are marked with A_W and A_E in Fig. 5. Only in region A_E where the orographic influence of the earth's topography could be considered relatively unimportant a detailed computation of both divergence and vertical velocity was performed, whereas in region A_W only the vertical velocity was computed for a few upper isobaric surfaces. In the eastern part a still smaller area, marked by A' and limited by the

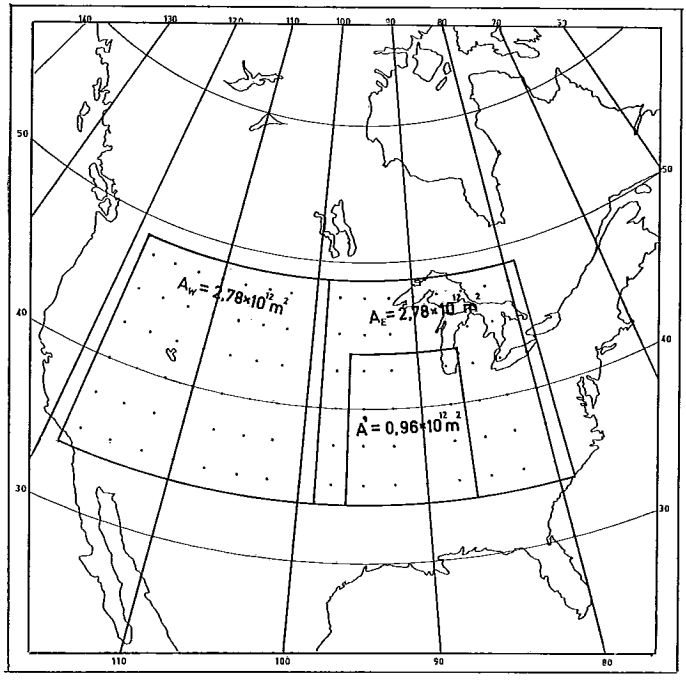

Fig. 5. Regions and grid points used for different computations.

latitudes 33.°75 and 43.°75 N and the longitudes 86.°25 and 96.°25 W, was especially selected; this region, about 0.96×10^{12} m^2 large, corresponds roughly to the central part of the cyclone and the principal precipitation area. In this smaller region the computed divergence was used for an estimate of the precipitation intensity for the corresponding synoptic time. The figure also contains the grid points, 2.5 degrees of latitude and longitude apart, for which divergence and vertical velocity were computed.

As the first step in the computation the zonal and meridional wind components u, v, for all stations were evaluated at standard levels. For region A_E these were plotted on separate maps for the isobaric levels 950, 900, 800, 700, 600, 500, 400, 300, 200 and 150 mb and a careful isotach analysis was made. From the isotach charts then the three terms in the expression for divergence.

$$\nabla \cdot \mathbf{v} = \frac{\partial u}{\partial x} + \frac{\partial v}{\partial y} - \frac{v}{a} \tan \varphi \tag{1}$$

were determined. Here a denotes the radius of the earth and φ the latitude. For the evaluation of Eq. (1) curves for u and v were drawn along selected parallels and meridians, and from these curves $\frac{\partial u}{\partial x}$ and $\frac{\partial v}{\partial y}$ were computed at the selected grid points in Fig. 5. The last term in formula (1), which is the correction term due to the convergence of the meridians, is generally if minor importance, but was always considered.

The two first terms in the above expression for divergence are often quite large, but appear with different signs. Hence relatively small errors and irregularities in the isotach analyses can result in quite large irregu-

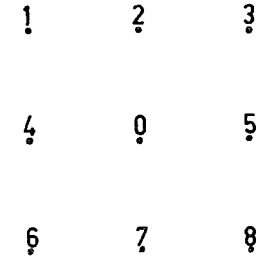

Fig. 6. Schematic figure explaining the smoothing of the divergence value at a point 0 by using 8 neighbouring points.

larities in the computed divergence which do not correspond to real variations. A method for smoothing the computed values was therefore applied before the divergence values were used. For this smoothing of the divergence at a given point the computed values in 8 neighbouring points (Fig. 6) were used and the final smoothed value in the central point was determined from the formula

$$(\nabla \cdot \mathbf{v})_0 = \frac{D_1 + D_3 + D_6 + D_8 + 2\,(D_2 + D_4 + D_5 + D_7) + 4D_0}{16}, \quad (2)$$

where D_i is the originally computed divergence at the point with the corresponding number i in the schematic figure. For the grid points at the boundary the divergence was evaluated at outer points not marked in Fig. 5. It is obvious that the smoothing results in a considerable reduc-

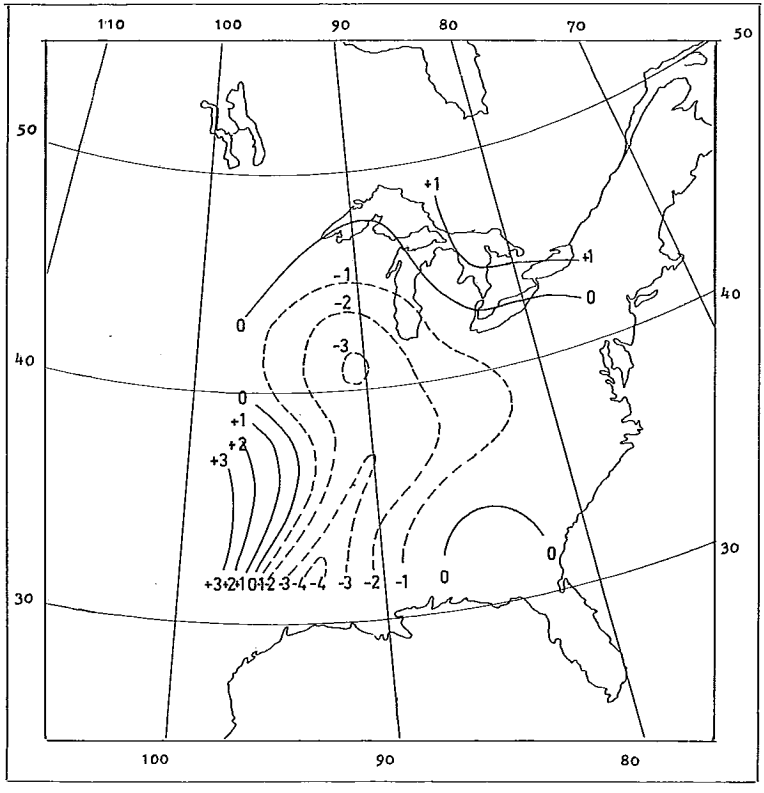

Fig. 7. Distribution of divergence (unit: 10^{-5} sec^{-1}) at 950 mb, Nov. 18, 1957, 1200 G.M.T.

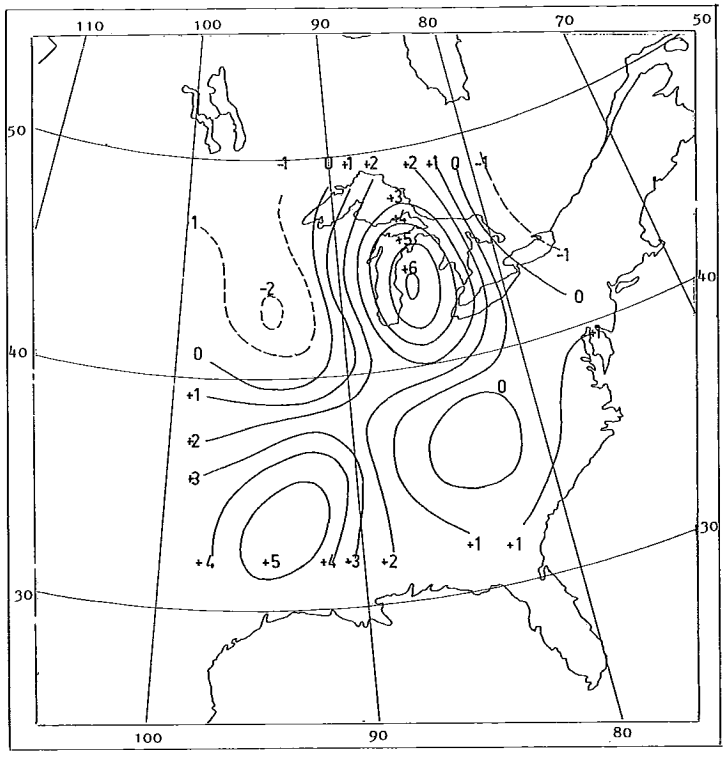

Fig. 8. Distribution of divergence (unit: 10^{-5} sec^{-1}) at 200 mb, Nov. 18, 1957, 1200 G.M.T.

tion of the divergence values near the centers of maximum or minimum divergence depending on the grid scale, but the available wind data are in no case so satisfactory that they would permit a detailed evaluation of the divergence field.

The smoothed values of the grid points gave the final distribution of divergence at the selected isobaric levels. Not all the charts are published here; only the maps for 950 mb and 200 mb are reproduced (Figs. 7—8). Of these the former map represents the divergence field in the lowest part of the region, whereas the 200-mb map gives the divergence in the vicinity of the tropopause. The mean divergence in the whole region was, at the 950-mb level, -0.60×10^{-5} sec^{-1} and, at the 200-mb level, 1.30×10^{-5} sec^{-1}. Hence the region was characterized by low-level convergence and high-level divergence, as could be expected for an essentially cyclonic region.

For the same grid points the vertical velocity was computed by using the simple formula

$$\frac{\partial \omega}{\partial p} = -\nabla \cdot \mathbf{v} \tag{3}$$

where $\omega = \frac{dp}{dt}$ denotes the vertical component of velocity in pressure coodinates. By integrating Eq. (3) the velocity at an arbitrary isobaric surface with pressure p_n can be determined from

$$\omega_{p_n} = \omega_{p_{n-1}} + \int_{p_n}^{p_{n-1}} \nabla \cdot \mathbf{v}\, dp \tag{4}$$

The smoothed divergence values for the grid points were used in the graphical integration. Further on it was assumed that the ω-values

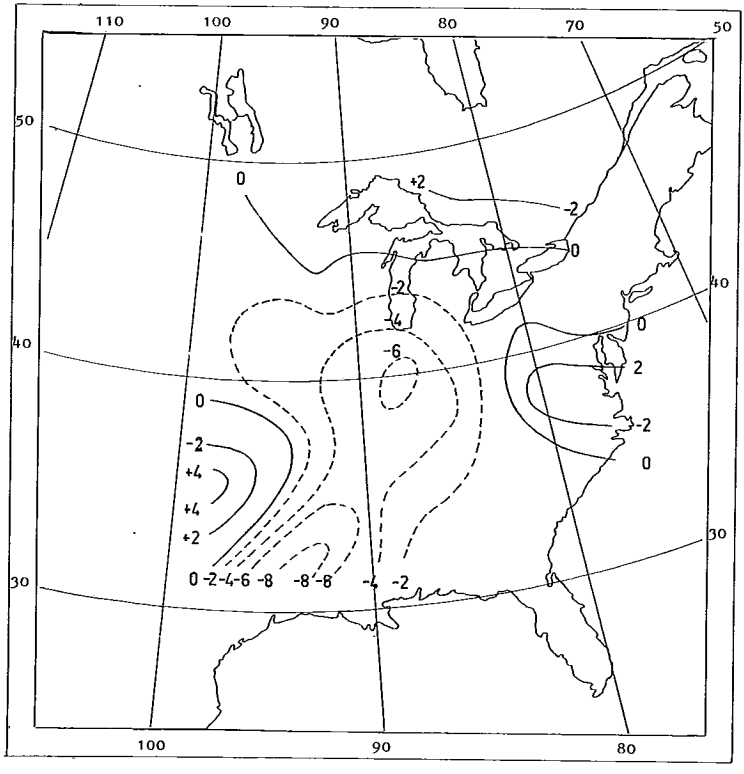

Fig. 9. Vertical velocity ω (unit: 10^{-4} cb sec^{-1}) at 700 mb, Nov. 18, 1957, 1200 G.M.T.

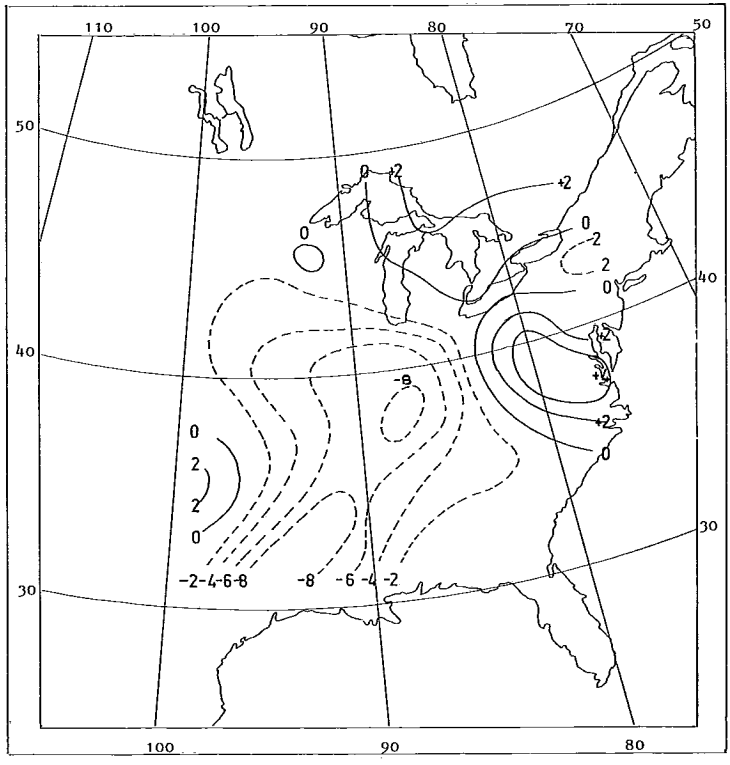

Fig. 10. Vertical velocity ω (unit: 10^{-4}cb sec^{-1}) at 500 mb, Nov. 18, 1957,1200 G.M.T.

disappeared at the lowest pressure surface p_0, corresponding to the average pressure at the ground in the whole region. This latter assumption is naturally not correct, but it can be shown that the errors following from this assumption are small compared with some of the other errors in our computation, as long as the topography of the earth's surface is relatively smooth.

The computed values of ω at the 700, 500 and 300 mb levels are presented in Figs 9—11. According to the charts ascending motion (negative ω-values) prevails in the central parts of the cyclone and along the cold front, whereas descending motion can be observed in the surroundings. The ascending motion seems to reach its highest values between 500 and 300 mb. In the central region of the cyclone, area A' in Fig. 5, the mean distribution of divergence and vertical velocity with pressure is presented in Fig. 12.

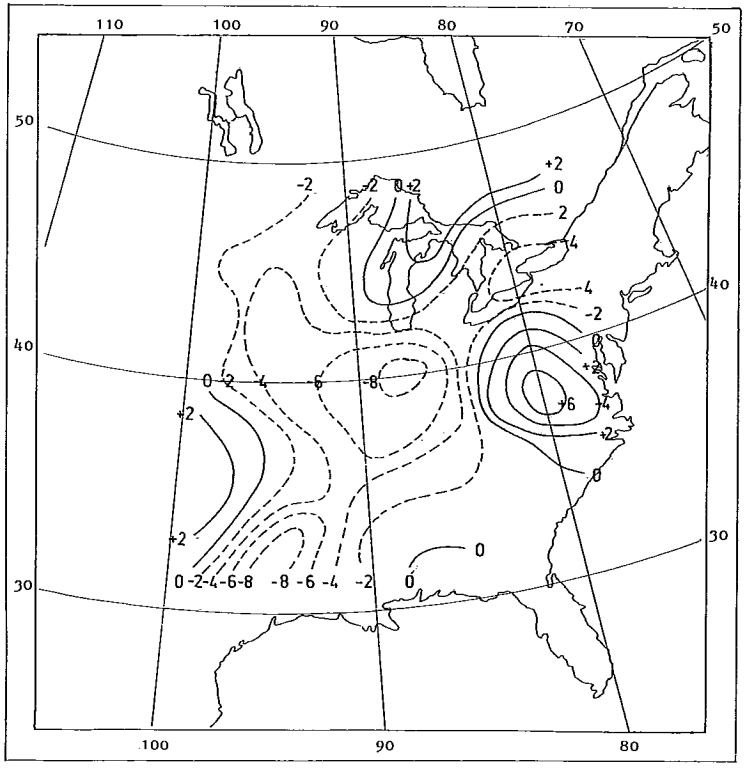

Fig. 11. Vertical velocity ω (unit: 10^{-4}cb sec^{-1}) at 300 mb, Nov. 18, 1957, 1200 G.M.T.

Because of the disturbing effects of the mountain regions in the western part, A_W, the divergence was not computed for this region for all the isobaric levels quoted above. To get values of the vertical motion in this part we applied another method used by several meteorologists (*e.g.* REX, [5]). Let p_s denote the pressure at the ground and p the pressure at an arbitrary level, then ω_p can be computed from

$$\omega_p = \frac{\partial U}{\partial x} + \frac{\partial V}{\partial y} - \frac{V}{a} \tan \varphi \,, \tag{5}$$

where:

$$U = \int_p^{p_s} u \, dp \,, \quad V = \int_p^{p_s} v \, dp \tag{6}$$

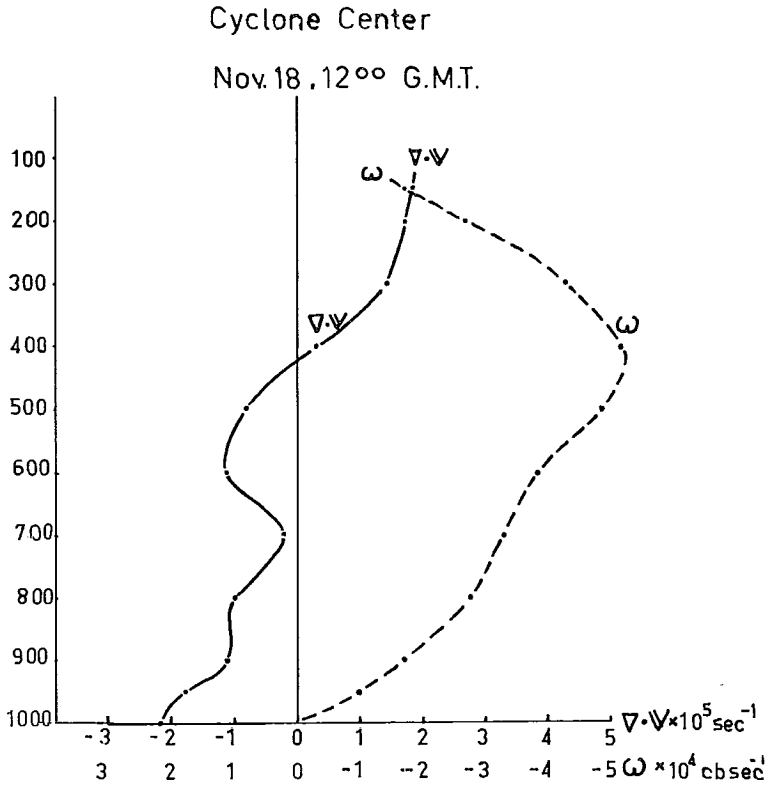

Fig. 12. Vertical distribution of mean divergence and vertical velocity in the central region of the cyclone, area A'in Fig. 5.

The same graphical method was used for evaluation of the terms in Eq. (5) as previously used in computing the divergence. An advantage in computing the ω-values directly from Eq. (5) lies in the use of mean wind components for deep atmospheric layers. The method implies therefore an elimination, at least to some extent, of small errors and short-time variations of the observed winds at fixed levels. On the other hand, however, our experience indicates that considerable errors in computing the terms in Eqs. (1) and (5) depend upon subjective errors in the isotach analysis. A large part of these errors can obviously be eliminated by the use of Eq. (4) since, except for the lowest levels, the ω-values are evaluated from several isotach analyses at different isobaric levels. By using Eq. (5), on the other hand, the ω-values depend only on one isotach analysis for

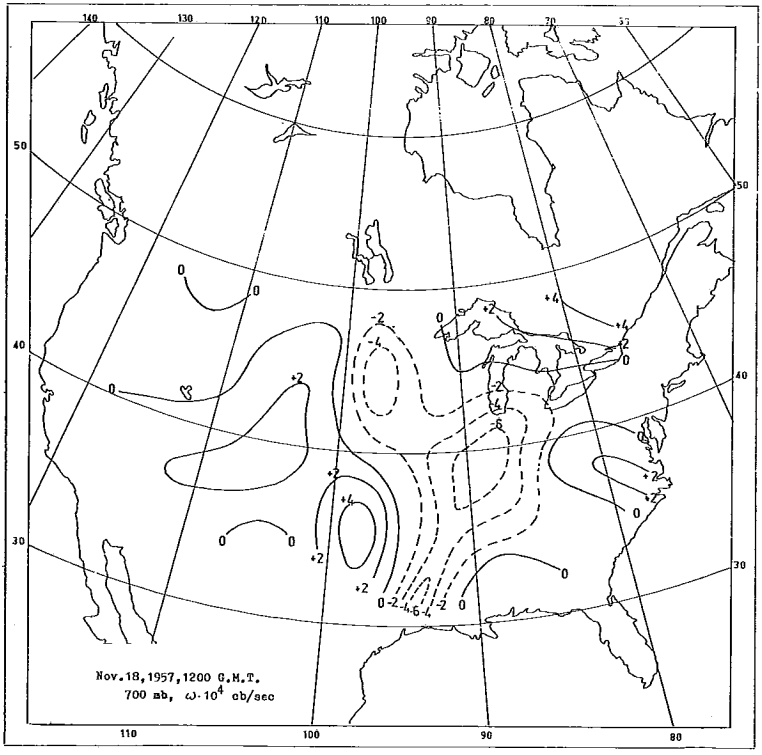

Fig. 13. Vertical velocity ω (unit: 10^{-4}cb $\sec^{-1}$) at 700 mb in the larger region, Nov. 18, 1957, 1200 G.M.T. In this and the two following figures the ω-values were computed from Eq. (5).

U and V with all its subjective errors. This latter method therefore necessarily results in a more erratic distribution of ω.

In Figs. 13—15 the distribution of the ω-values in the whole larger region, $A_W + A_E$, at the levels 700, 500 and 300 mb is presented. Again no attempt was made to eliminate the orographic effect which obviously must be quite large over the western part. A comparison with the corresponding charts in Figs 9—11 shows a good agreement in the corresponding areas for the 700-mb chart, but at higher levels Figs. 14 and 15 show a considerably stronger upward motion than the corresponding charts in Figs. 10—11. It would have been possible to reanalyze the isotach charts for u, v and U, V to achieve a better agreement; however,

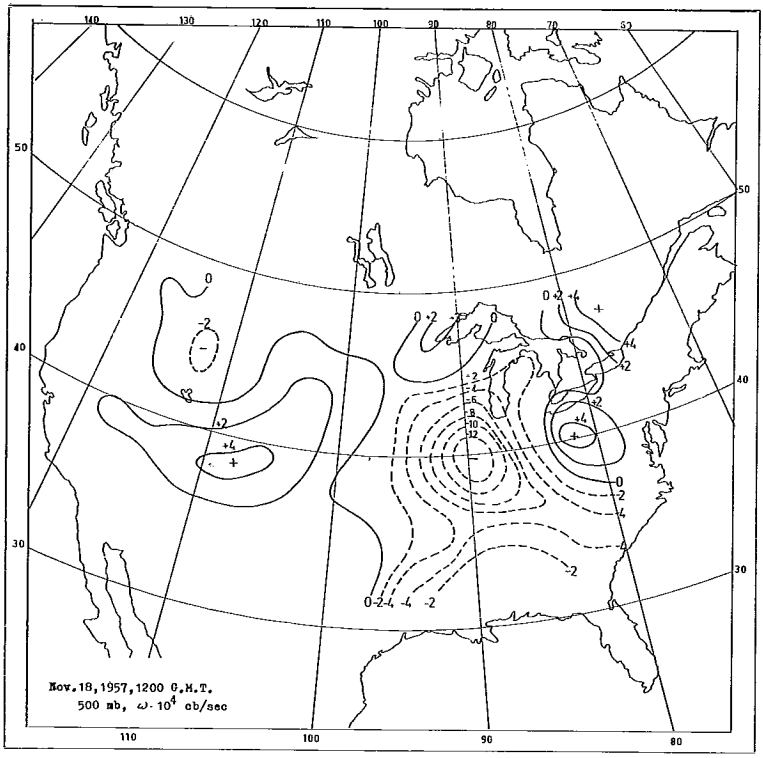

Fig. 14. Vertical velocity ω (unit: 10^{-4}cb $\sec^{-1}$) at 500 mb, Nov. 18, 1957,1200 G.M.T.

no such attempt was made. We feel, however, that the ω-distribution in Figs 9—11 are somewhat more reliable than the corresponding distribution in Figs 13—15.

3. *Field of Divergence and Precipitation*

The intensity of precipitation in the central parts of the cyclone can be used for an estimate of divergence and vertical velocity, and, vice versa, the computed values of divergence and vertical velocity can be utilized to compute the precipitation. If then the computed precipitation closely agrees with the measured rainfall the divergence values cannot be very wrong.

Let P denote the rate of precipitation per unit area, E the rate of evaporation from the ground and q the specific humidity. If we assume

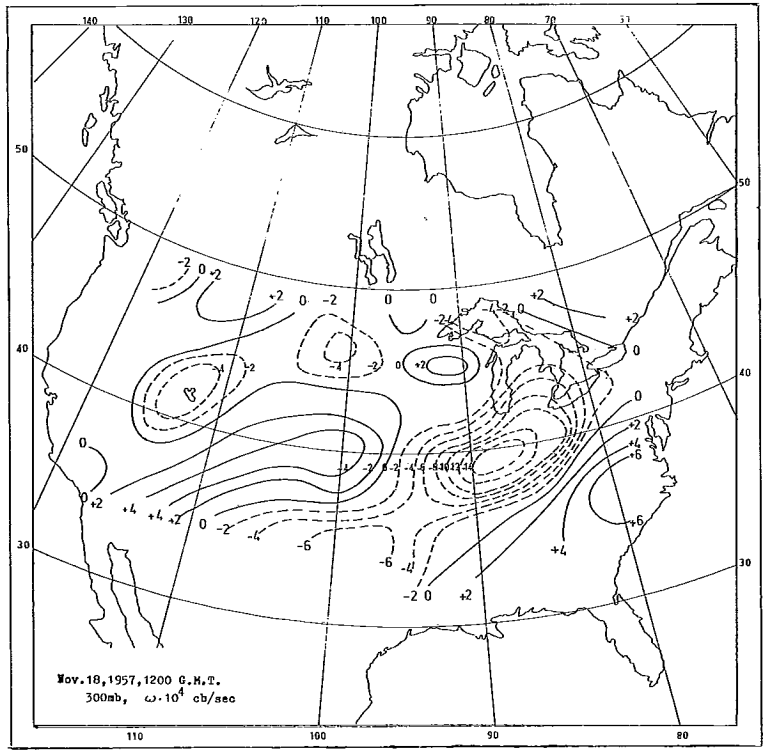

Fig. 15. Vertical velocity ω (unit: 10^{-4}cb $\sec^{-1}$) at 300 mb, Nov. 18, 1957,1200 G.M.T.

that the condensed water immediately precipitates, P can be computed from:

$$P = E - \frac{1}{g}\int_0^{p_0} \frac{\partial q}{\partial t}\, dp - \frac{1}{g}\int_0^{p_0} \nabla \cdot (q\,\mathbf{v})\, dp \qquad (7)$$

The last assumption is not even approximately valid for small regions, and the small-scale divergence field cannot be determined from wind observations on the regular synoptic stations. Further, the instantaneous precipitation intensity should be replaced by the mean intensity over a limited time period in any such comparison with the computed precipitation, especially since, in the selected synoptic case, at least part of the rainfall, came as showers. Satisfactory agreement between the computed and observed precipitation can therefore be expected only if

the comparison is made for a relatively large region and extended over a certain time centred around the synoptic period.

Eq. (7) can thus be averaged in to the form

$$\bar{P} - \bar{E} = -\frac{1}{g}\int_0^{p_0} \overline{\frac{\partial q}{\partial t}}\, dp - \frac{1}{g}\int_0^{p_0} \overline{\mathbf{v}\cdot\nabla q}\, dp - \frac{1}{g}\int_0^{p_0} \overline{q\nabla\cdot\mathbf{v}}\, dp\,. \tag{8}$$

In cases of no divergence or lower divergence and upper convergence (descending motion) P either vanishes or is quite negligible. In such cases evaporation E from the ground can be computed either from Eq. (7) or (8). Considering especially the non-divergent case we get

$$\bar{E} \approx \frac{1}{g}\int_0^{p_0} \overline{\frac{\partial q}{\partial t}}\, dp + \frac{1}{g}\int_0^{p_0} \overline{\mathbf{v}\cdot\nabla q}\, dp\,. \tag{9}$$

Since E in a cyclonic situation with heavy precipitation must be small compared to P we can therefore conclude that the sum of the two first right-hand terms in Eq. (8) generally must be small compared with the last term. This conclusion is especially true if the atmosphere in lower levels is nearly saturated, which could be expected in the central precipitation area. Hence the rate of precipitation in such cases can be approximately computed from the simple formula

$$\bar{P} \approx -\frac{1}{g}\int_0^{p_0} \overline{q\nabla\cdot\mathbf{v}}\, dp\,. \tag{10}$$

For the case November 18, 1957, 1200 G.M.T. the central region of the cyclone had quite intense precipitation and was therefore selected for the computation of $\bar{P}$. The region is marked by A' in Fig. 5 and its area was 95.9×10^{10} m^2. The area A' contained 16 gridpoints for which the smoothed values of $\nabla\cdot\mathbf{v}$ were computed at the selected isobaric surfaces. No attempt was made to compute the local change of the water vapor content in the region, but it was assumed to be small at the synoptic time in question. The mean observed precipitation over the total area was computed from the hourly data of precipitation published by the U.S. Weather Bureau for the period of 6 hours from 0900—1500 G.M.T. The mean amount of precipitation in the area was 7.6 mm or 7.6 kg water per m^2. Assuming no change of the divergence field during the 6 hour period and extending the computation from the mean ground

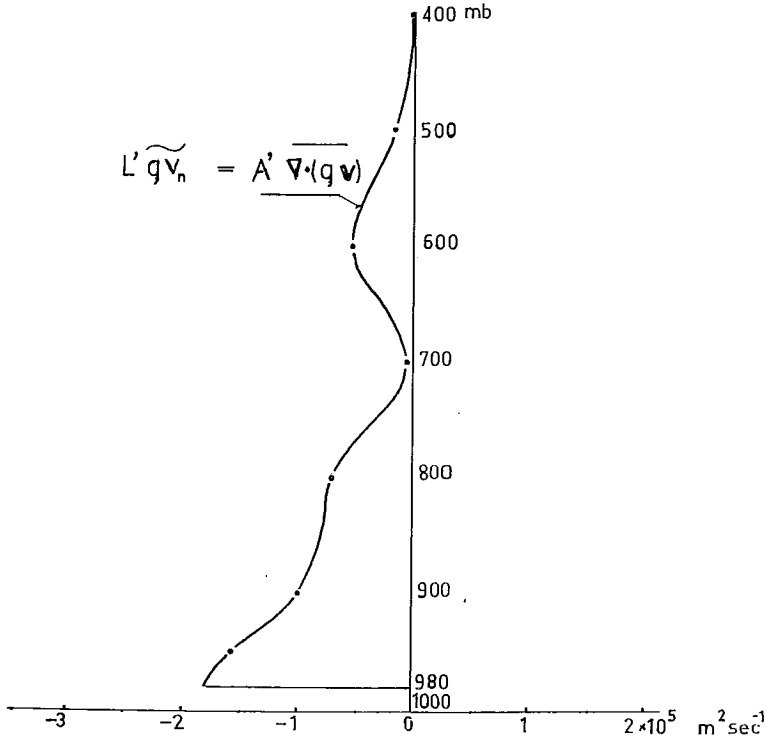

Fig. 16. Graphical method for computation of the total influx of water vapor into the region A' and the corresponding mean precipitation intensity.

pressure 980 mb to the 400-mb surface, the graphical evaluation gave the following results:

$$-\frac{1}{g}\int_{40\ cb}^{98\ cb} \overline{\nabla_p \cdot (q\,\mathbf{v})}\, dp = 7.4 \text{ mm/6 h}$$

$$-\frac{1}{g}\int_{40\ cb}^{98\ cb} \overline{q\,\nabla \cdot \mathbf{v}}\, dp = 6.2 \text{ mm/6 h}$$

The integration was extended only to 400 mb because of the low q-values at higher levels (Fig. 16).

The agreement between computed and observed precipitation over the whole area A' must be considered excellent. The difference between the

observed precipitation and the precipitation computed from the divergence, 1.4 mm/6 h, can be considered as the sum of the three terms:

$$E - \frac{1}{g}\int_{40}^{98} \frac{\partial q}{\partial t}\, dp - \frac{1}{g}\int_{40}^{98} \mathbf{v} \cdot \nabla_p\, q\, dp$$

in Eq. (8). Of these terms E obviously is positive, but a mean rate of evaporation from the ground of 1.2 mm per 6 hours would be much too large. Hence the sum of the two other terms contributes to the precipitation. However, whether the difference wholly depends upon the neglection of the three minor terms in Eq. (8) or partly upon errors in the computation of $\nabla \cdot (q\,\mathbf{v})$ and $q\nabla \cdot \mathbf{v}$ is hard to decide. In any case, one can conclude that the mean values of the computed divergence in region A' for different isobaric levels cannot be too wrong.

The mean release of latent heat over the area A' during the 6 hour-period amounts to 46×10^5 calories per m^2, which corresponds to a rate of release of 2.1×10^2 cal/m^2 sec or 87.9×10^{-2} kj/m^2 sec. The value may be compared with the solar constant of 3.3×10^2 cal/m^2 sec. The total release of latent heat over the area A' amounts to 201×10^{12} calories or 84.1×10^{10} kilojoules per second.

4. *Energy Conversions*

We shall now consider the total volume over the area A between the surface pressure and a fixed isobaric surface with the pressure p_h. If the length of the boundary of A is denoted by L the time rate of change of the total kinetic energy in the volume considered is determined by:

$$\frac{A}{g}\frac{\partial}{\partial t}\int_{p_h}^{p_0} \overline{k}\, dp = -\frac{L}{g}\int_{ph}^{p_0} \widehat{k\, v_n}\, dp + \frac{A}{g}\,\overline{[k\omega]}_{p_h} - \frac{A}{g}\int_{p_h}^{p_0} \overline{\mathbf{v} \cdot \nabla\, \Phi\, dp} +$$

$$+ A\int_0^h \left(\overline{u\frac{\partial \tau_{xz}}{\partial z}} + \overline{v\frac{\partial \tau_{yz}}{\partial z}}\right) dz\,. \tag{11}$$

Here k denotes the kinetic energy per unit mass, v_n is the normal component of the wind across the boundary L, $\Phi = gz$ is the geopotential, and τ_{xz}, τ_{yz} are the zonal and meridional components of the shearing stress due to variation of wind with height. In the equation the horizontal

bars denote areal mean values, whereas the circumflex denotes a mean value along the boundary L.

In Eq. (11) the first term on the right hand side gives the total flux of kinetic energy through the vertical boundary, whereas the second term represents the flux across the isobaric surface p_h. The third term represents the production of kinetic energy due to cross-isobaric flow, and the last term gives the frictional dissipation of kinetic energy.

Eq. (11) can (PALMÉN, [3]) be transformed into:

$$\frac{A}{g}\frac{\partial}{\partial t}\int_{p_h}^{p_0}\overline{k}\,dp = -\frac{L}{g}\int_{p_h}^{p_0}\widehat{k}\,\widehat{v_n}\,dp + \frac{A}{g}\overline{[k\omega]}_{p_h} - \frac{L}{g}\int_{p_h}^{p_0}(\hat{\Phi}-\bar{\Phi})\,\widehat{v_n}\,dp -$$

$$-\frac{L}{g}\int_{p_h}^{p_0}\widehat{\Phi''}\,\widehat{v_n''}\,dp + \frac{A}{g}\overline{[\Phi'\omega']}_{p_h} - \frac{AR}{g}\int_{p_h}^{p_0}\frac{\overline{T'\omega'}}{p}\,dp - A\,\overline{\varkappa\varrho_0\,V_0^3} - \tag{12}$$

$$-A\int_0^h\overline{\mu\left[\left(\frac{\partial u}{\partial z}\right)^2+\left(\frac{\partial v}{\partial z}\right)^2\right]}\,dz$$

Here $'$ denotes the deviation from the areal mean value and $''$ the deviation from the mean value at the bounary L, R is the gas constant, T the Kelvin temperature, $\varkappa$ the drag coefficent at the surface, ϱ_0 and V_0 are the density of air and wind velocity at »anemometer height» and μ is the coefficient of eddy viscosity in the atmosphere.

In the above equation $\hat{\Phi}-\bar{\Phi}$ and Φ'' are small quantities compared with Φ. The first two right-hand terms represent the horizontal and vertical flux of kinetic energy across the bounding surface, the third and fourth terms represent the work done by the inside volume on the surrounding atmosphere, the fifth term can be considered as the vertical flux of potential energy across the isobaric surface p_h, the sixth term represents the conversion between potential and kinetic energy inside the volume, the seventh term the dissipation of kinetic energy due to surface friction, and the last term the frictional dissipation in the atmosphere.

An attempt was made to compute all these terms for the whole area A, 556×10^{10} m^2 large, indicated in Fig. 5, by using the values of ω in Figs 13—15 and the corresponding values of u, v, and T. In evaluating the surface friction a mean value for $\varkappa$ of 0.005 was used. For ocean surfaces it has generally been assumed that $\varkappa$ could vary between 0.0015

and 0.0025, but for continental regions much higher values must be considered. For a more or less plane continental surface a value of 0.005 perhaps could be assumed; however, considering the mountains over the western part of the selected region, higher mean values should be expected. Therefore it is probable that the mean value 0.005 is too low and the computed frictional dissipation hence too small[1]). No attempt was made to evaluate the frictional dissipation in the atmosphere (last term in Eq. (12)). The vertical integration was extended between the mean pressure at the ground, 95 cb, and 30 cb.

The evaluation of the different terms in Eq. (12) gave the following results:

$$-\frac{L}{g}\int_{30}^{95}\widehat{kv_n}\,dp = 8.8 \times 10^{10}\ \text{kj/sec}$$

$$\frac{A}{g}\,[\overline{k\omega}]_{30} = -9.8 \times 10^{10}\ \text{»}$$

$$-\frac{L}{g}\int_{30}^{95}(\hat{\Phi}-\overline{\Phi})\hat{v}_n dp = 4.3 \times 10^{10}\ \text{»}$$

$$-\frac{L}{g}\int_{30}^{95}\widehat{\Phi'' v_n''}\,dp = 1.1 \times 10^{10}\ \text{»}$$

$$\frac{A}{g}\,[\overline{\Phi'\omega'}]_{30} = -5.9 \times 10^{10}\ \text{»}$$

$$-\frac{AR}{g}\int_{30}^{95}\frac{\overline{T'\omega'}}{p}\,dp = 11.7 \times 10^{10}\ \text{»}$$

$$-\overline{A\,\varkappa\varrho_0\,V_0^3} = -0.6 \times 10^{10}\ \text{»}$$

The total sum of the seven terms is 9.6×10^{10} kj/sec. As already mentioned, the frictional dissipation in the atmosphere between 950 and

[1]) According to a recent study by CRESSMAN [1] the mean drag coefficient in region A could easily be twice as large as assumed here.

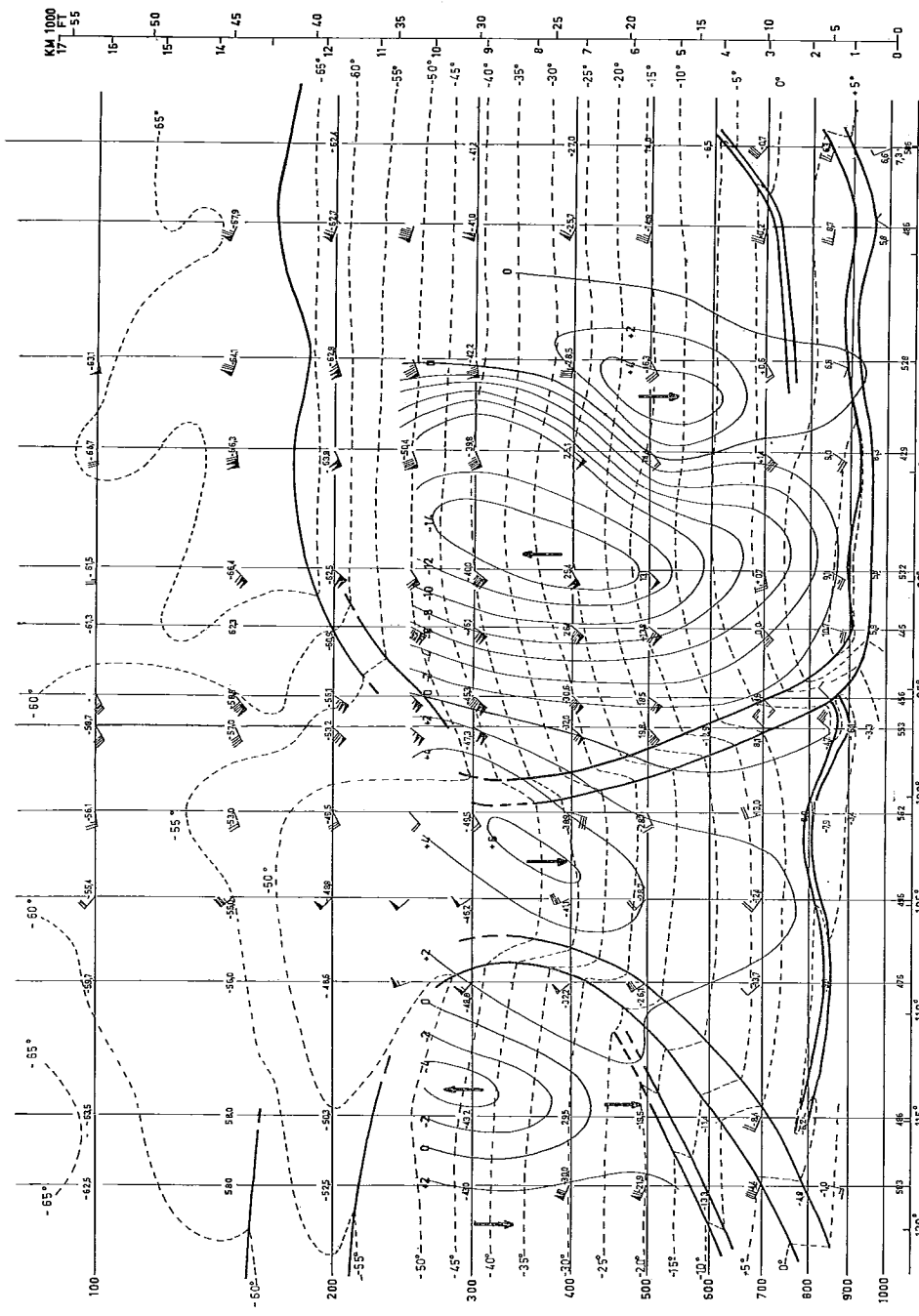

Fig. 17. Zonal cross-section along latitude 40°N, Nov. 18, 1957, 1200 G.M.T. Thick solid lines represent frontal boundaries, inversions or tropopauses, thin solid lines mark isotach values for ω (unit: 10^{-4}cb sec^{-1}) and thin dashed lines isotherms.

300 mb, and in addition, the small drag at the 300 mb level, have been disregarded. If, for this dissipation, we assume the same value as for the surface dissipation, the kinetic energy of the whole volume of the atmosphere considered in the computation should increase at the rate 9.0×10^{10} kilojoules per second. The frictional dissipation thus estimated at only 1.2×10^{10} kj/sec seems surprisingly small compared with the other terms in Eq. (12). In this situation no really very strong winds were observed on the surface map, and over large areas the surface winds were weak. On the other hand, there was a strong vertical wind shear, and therefore it is probable that the atmospheric dissipation of kinetic energy was considerably larger than our estimated value.

The total kinetic energy of the whole region up to 300 mb was for the synoptic time evaluated to be 85.4×10^{14} kilojoules. An increase of 9.0×10^{10} kj/sec^{-1} corresponds to a total increase of 38.9×10^{14} kilojoules in 12 hours, which corresponds to about 46 per cent of the existing kinetic energy. Such an increase seems somewhat too high. It would roughly correspond to an increase of the average wind by about 20 per cent. However, an extension of the time rate of 9.0×10^{10} kj/sec over a 12 hours period is probably not permissible. On the other hand, the synoptic time selected for the computation was characterized by strong deepening of the surface cyclone, as can be seen from the consecutive surface maps. It should also be stressed that the evaluation of the different terms in Eq. (12) was performed by using the ω-values at only three isobaric surfaces and that the vertical velocity over the center of the cyclone probably represented an overestimate as can be seen by a comparison with the values in Figs 9—11.

The large value of the sixth right-hand term in Eq. (12) which gives the conversion between available potential and kinetic energy inside the region A shows that an important role in the deepening of the cyclone was played by ascent of warm air and descent of cold air. This process of solenoidal circulation occured essentially in a zonal plane, as can be seen from the vertical cross section in Fig. 17. The total rate of conversion, 11.7×10^{10} kilowatts, corresponds to a mean value of 210×10^{-4} kj/m^2 sec. By using a simple atmospheric model for coputing the vertical velocities from the vorticity equation WHITE and SALTZMAN [6] some years ago estimated the mean rate of conversion between potential and kinetic energy during January 1953 in almost the same region to be 50×10^{-4} kj/m^2 sec which is less than a quarter of our value for November 18, 1957. By using a similar simple model WIIN-NIELSEN [7] recently

estimated the rate of conversion during January 1959 for a large part of the northern hemisphere to be 16×10^{-4} kj/m^2 sec, whereas PALMÉN [3] by using the same model for the period January 1—4, 1956 computed the rate of conversion to be 22×10^{-4} kj/m^2 sec.

The special cyclone selected for our computation must be considered a rather extreme case with much stronger energy conversion than that which, on the average, occurs in the region of the U.S. However, in the case of cyclone »Hazel» in October 15, 1954 the conversion was considerably stronger amounting to a rate of 720×10^{-4} kj/m^2 sec (PALMÉN, [2]) over a somewhat smaller total area. The »Hazel» case was one of the most vigorous cyclone developments observed over the U.S.

It should be stressed once more that the evaluation of the different terms in the energy equation necessarily contains serious errors. Such errors cannot fully be avoided with the wind data available. It is possible that some of the errors depending upon the subjectivity in the isotach analysis of the wind field could be eliminated by some kind of objective analysis. On the other hand, the results as a whole show that both the divergence field and the vertical wind field computed from wind observations give a realistic picture of atmospheric processes essential for an understanding of important weather phenomena and the nature of the atmospheric energy conversions.

One more conclusion could be drawn from the energy computation. From the intensity of precipitation the release of latent heat in the warm air east of the upper trough was estimated to be 201×10^{12} calories or 84×10^{10} kilojoules per second. Obviously this additional source of heat in the ascending warm air essentially contributed to the maintenance of the energy-producing vertical-circulation. A similar distribution of the release of latent heat can be observed in most vigorous extratropical disturbances. Since the latent heat in developing young cyclones essentially is liberated in the ascending warm air masses the contribution of this strong energy source must be considered to be of great importance for the conversion processes between potential and kinetic energy. In most dynamic theories of recent years the latent heat has been neglected or considered of minor importance. In that respect a correction obviously has to be made.

REFERENCES

1. CRESSMAN, G. P., 1960: Improved terrain effects in barotropic forecasts. *Mon. Weath. Rev.*, **88**, 327—342.
2. PALMÉN, E., 1958: Vertical circulation and release of kinetic energy during the development of hurricane Hazel into an extratropical storm. *Tellus* **10**, 1—23.
3. —»— 1960: On generation and frictional dissipation of kinetic energy in the atmosphere. *Soc. Scient. Fennica, Comm. Phys.-Math.* XXIV, *11*, 15 pp.
4. PANOFSKY, H. A., 1951: Large-scale vertical velocity and divergence. *Compendium of Meteorology*, American Meteor. Soc., Boston, Mass., 639—646.
5. REX, D. F., 1958: Vertical atmospheric motion in the Equatorial Central Pacific. *Geophysica*, **6**, 479—500.
6. WHITE, R. M. and B. SALTZMAN, 1906: On conversion between potential and kinetic energy in the atmosphere. *Tellus*, **8**, 357—363.
7. WIIN-NIELSEN, A., 1959: A study of energy conversion and meridional circulation for the large-scale motion in the atmosphere. *Mon. Weath. Rev.*, **87**, 319—332.